scientific reports

Check for updates

OPEN

Laminar fluid ejection device enables high yield and preservation of mRNA and SaRNA LNP formulations

Chia Hao Ho[1,2], Irafasha C. Casmil[1,2], Manu Sharma[3], Tim Rees[3], Kenza Enright[3], Nick Allan[4] & Anna K. Blakney[1,2]✉

The development of messenger RNA (mRNA) and self-amplifying RNA (saRNA) vaccines has revolutionized modern vaccinology, particularly with the success of lipid nanoparticle (LNP)-based SARS-CoV-2 vaccines. Intranasal administration offers a promising approach for respiratory vaccines, providing mucosal immunity at the primary entry site of pathogens. However, the impact of different aerosolization delivery systems on RNA-LNP stability, recovery volume and functionality is not well understood. In this study, we compare the effects of three intranasal administration devices- a commercial Nebulizer, a commercial Spray, and a Laminar Fluid Ejection (LFE) Device developed by Rocket Science Health- on LNP physicochemical properties, RNA encapsulation efficiency, and functional protein expression level. Our findings demonstrate that high shear forces in the commercial nebulizer delivery system significantly increase LNP particle size (85 nm to 300 nm) and polydispersity index (PDI), leading to RNA degradation and reduced encapsulation efficiency (100–39%). Conversely, the LFE Device preserved LNP structural integrity, achieving the highest RNA encapsulation efficiency (94% for mRNA, 102% for saRNA) and superior functional protein expression (3-fold higher luciferase activity compared to the CM Nebulizer). These results highlight the importance of selecting an appropriate delivery system to optimize RNA-LNP delivery and retention in intranasal applications. Our study supports the LFE Device as a viable candidate for effective RNA-LNP-based mucosal vaccine administration, with potential applications in next-generation RNA therapeutics.

Keywords Intranasal RNA-LNP delivery, Aerosolization systems, Self-Amplifying RNA (saRNA), Lipid nanoparticles (LNPs), Mucosal vaccine efficacy

The COVID-19 pandemic has highlighted the potential of synthetic messenger RNA (mRNA) as a vaccine platform, bringing it to the forefront of global biomedical research. The rapid development, production, and distribution of mRNA-LNP vaccines, spearheaded by Moderna and Pfizer/BioNTech, demonstrated the transformative impact of RNA therapeutics and underscored the importance of lipid nanoparticle (LNP) delivery systems in modern vaccinology[1]. While we know that the highly transmissible SARS-CoV-2 (COVID-19) infects the respiratory tract and spreads through respiratory droplets and aerosols, only seven out of nearly a hundred COVID-19 vaccines are delivered intranasally[2]. A recent study using adenoviral vectors demonstrated that intranasal vaccination induces superior mucosal immunity, enhances lung tissue-resident memory T cells, and strengthens trained innate immunity, providing more effective protection against SARS-CoV-2 infection compared to traditional intramuscular vaccination[3]. Another study also showed that the intranasal administration of mRNA-LNP vaccines in Syrian golden hamsters induced robust systemic and mucosal immune responses, effectively reducing the viral loads and lung pathology[4]. LNPs play a critical role in protecting RNA from degradation by extracellular RNases and facilitate the intracellular delivery[5]. Among various administration routes for LNP-formulated RNA therapeutics, intranasal delivery offers distinct advantages, including reducing the systemic immunogenicity, bypassing the liver clearance for prolonged expression, and eliminating the need for needle-based injections. Notably, intranasal administration can effectively induce strong immune responses against respiratory viruses such as SARS-CoV-2, making it a promising strategy for vaccine development[6]. However,

[1]Michael Smith Laboratories, University of British Columbia, Vancouver, BC, Canada. [2]School of Biomedical Engineering, University of British Columbia, Vancouver, BC, Canada. [3]Rocket Science Health, Victoria, BC, Canada. [4]StarFish Medical, Victoria, BC, Canada. ✉email: anna.blakney@msl.ubc.ca

a key challenge in intranasal administration of RNA-LNPs is producing small droplets without subjecting the particles to excessive mechanical stresses (i.e. shear stress, osmotic pressures a and interfacial forces), which can disrupt LNP integrity, expose RNA to the outside environment, and lead to degradation by RNases[6–8].

Intranasal administration devices, such as some pressurized nasal sprays, dispense and eject fluid using compressed air through atomizing mechanisms[9]; however, not all use compressed air-some use a refrigerant as a propellant[10], and there are other physical mechanisms as well[11]›. This process generates turbulent droplets that predominantly disperse throughout the lower nasal passages rather than reaching the upper nasal cavity, limiting effective mucosal delivery[12]. Additionally the high velocity airflow through the nasal valve can destroy the cargo and cause degradation[12]. Another common intranasal delivery method is the vibrating membrane nebulizer, which utilizes a flexible mesh-like membrane attached to a piezoelectric ring actuator or ultrasound transducer. This actuator vibrates at an extremely high frequency, expelling droplets with sizes ranging from 1 to 10 µm, optimizing aerosol generation for effective respiratory delivery[13]. While this method has been shown to preserve the integrity of SARS-CoV-2 mRNA vaccines for respiratory delivery, studies have primarily focused on shorter mRNA sequences[6].

Longer mRNA molecules, such as self-amplifying RNA (saRNA), represent a next-generation RNA technology capable of expressing heterologous genes derived from alphaviruses[14]. saRNA includes sequences encoding a replicase complex, which comprises non-structural proteins nsP1 through nsP4 that facilitate amplification[14]. Upon delivery into the cytoplasm, the replicase is translated and initiates replication of the saRNA, leading to the production of a subgenomic RNA that directs the synthesis of the target antigen[15]. This platform offers prolonged protein expression and requires lower dosages compared to conventional mRNA, making it a promising advancement in RNA-based therapeutics and vaccines[16]. saRNA-based vaccines (ARCT-154) have received regulatory approval for COVID-19 in Japan and the European Union[17,18]. While the ARCT-154 saRNA vaccine is currently administered intramuscularly, one study has demonstrated that saRNA expression in vivo can also be achieved through intranasal delivery[19]. This finding expands the potential applications of saRNA technology in RNA therapeutics by offering a non-invasive route of administration that could enhance mucosal immunity and broaden vaccine accessibility. However, due to their longer strand length, saRNA may be more vulnerable to degradation when exposed to high mechanical forces in the intense environment of aerosolization[6].

Recently, a novel intranasal drug delivery system known as the laminar fluid ejection (LFE) device was developed. While originally designed to enable precise targeting of the olfactory cleft—an optimal site for particle deposition in certain drug delivery contexts—its unique delivery mechanism offers potential for adaptation toward targeting immunologically relevant regions of the nasal cavity[12]. In this study, we investigated the utility of the LFE device for RNA-LNP delivery and intranasal vaccination. Aspects of the LFE device used in this study are covered by U.S. Patent No. 11,497,862 and related pending applications. By directly ejecting fluid from the reservoir as a controlled stream into the nasal cavity, this approach minimizes mechanical forces, enhances dosing consistency, and reduces dead volume, making it a promising advancement for RNA-LNP delivery[12]. In this study, we conducted a comprehensive comparison of three different intranasal administration devices, including a vibrating membrane nebulizer, nasal spray, and laminar fluid ejection (LFE) device. We investigate how the devices impact RNA-LNP integrity and delivery efficiency. Beyond characterizing the physicochemical properties of LNPs, such as particle size, uniformity, and surface charge, we assess the effects of aerosolization on RNA recovery percentage and encapsulation efficiency. Furthermore, we assess how different dispensing processes impact the biological activity of RNA-LNPs by measuring luciferase protein expression in vitro. Additionally, we investigate both mRNA-LNP and saRNA-LNP, a novel self-amplifying RNA-LNP platform previously developed in our lab, to further explore its potential for next-generation RNA vaccines and therapeutics[20].

Materials and methods

Plasmids.

The self-amplifying RNA (saRNA) backbone used in this study was derived from the Venezuelan equine encephalitis virus (TC83 strain; GenBank Accession no. L01443), with firefly luciferase (Fluc) as a reporter protein (UniProt ID: P08659). The mRNA Pfizer-BioNTech plasmid (pUC-5'P3'P) was kindly provided by Dr. Andrew Varley from the University of British Columbia RNA Core. The firefly luciferase (Fluc) gene, used as a reporter protein, was cloned into the plasmid using the NEBuilder HiFi DNA Assembly Kit (NEB) following the manufacturer's instructions and protocols. All plasmids were transformed into *E. coli* DH5α cells (New England Biolabs) and plated on LB agar plates containing 50 µg/mL ampicillin. Plates were incubated overnight at 37 °C. A single colony was selected and subjected to Sanger sequencing to confirm the correct cloning of saRNA-Fluc and mRNA-Fluc constructs. After sequence verification, glycerol stocks were prepared, and the confirmed plasmids were cultured overnight at 37 °C with 225 rpm shaking in 200 mL of LB broth containing 50 µg/mL ampicillin (Gibco, Thermo Fisher Scientific). The Qiagen® Plasmid Plus Maxi Prep kit (QIAGEN, US) was utilized for isolating the plasmid according to the manufacturer's protocol.

In vitro transcription of saRNA and mRNA.

The saRNA-Fluc and mRNA-Fluc plasmids were linearized using SapI restriction enzyme (NEB) at a final concentration of 125 µg/mL. The reaction was incubated at 37 °C for 2 h, followed by enzyme inactivation at 65 °C for 20 min. The linearized DNA was then purified and used as a template for subsequent in vitro transcription (IVT) following previously optimized protocols established in our lab[21]. The IVT reaction was conducted using an Eppendorf ThermoMixer C to ensure precise temperature control. The IVT master mix contained the following components: 1 M Tris-HCl buffer solution (Sigma-Aldrich), 1 M magnesium acetate (Sigma-Aldrich), spermidine (Thermo Fisher Scientific), dithiothreitol (Thermo Fisher Scientific), unmodified nucleotide triphosphates (Thermo Fisher Scientific), T7 RNA polymerase (NEB), murine RNase inhibitor (NEB), pyrophosphatase (NEB), and ultrapure DNase/RNase-free water (Thermo Fisher Scientific). The linearized

saRNA template was mixed with the IVT master mixture and incubated at 30 °C for 2 h with gentle shaking to facilitate the process. mRNA was synthesized following the same procedure and using the same reagents as the saRNA IVT reaction. However, instead of unmodified nucleotide triphosphates, uridine-5′-triphosphate (UTP) was replaced with N1-methylpseudouridine-5′-triphosphate (m1Ψ-5′-triphosphate) (Hongene). The mRNA IVT reaction was conducted at 37 °C for 2 h under gentle shaking. Post-transcriptional capping of both saRNA and mRNA was performed using the CellScript Cap-1 System (CellScript) to enhance RNA stability and translational efficiency. Following capping, all RNA samples were purified using the Monarch RNA Cleanup Kit (NEB) according to the manufacturer's protocol.

LNP Formulation.

Lipid nanoparticles (LNPs) were formulated using a rapid T-tube mixing method, where RNA in pH 4.53 sodium acetate buffer (Millipore Sigma) was combined with a lipid mixture in a 100% ethanol phase[20]. The mixing was performed using the Pump 33 DDS Syringe Pump (Harvard Apparatus) at a total flow rate of 20 mL/min with a flow rate ratio of 3:1 (RNA: lipid) and a nitrogen-to-phosphate (N: P) ratio of 6. The lipid formulation for both mRNA and saRNA consisted of a molar ratio of 46.3:9.4:42.7:1.6 of ALC-0315 ((4-hydroxybutyl) azanediyl)di(hexane-6,1-diyl) bis(2-hexyldecanoate) (BroadPharm), DSPC (1,2-dioleoyl-sn-glycero-3-phosphoethanolamine) (Avanti Polar Lipids), plant-derived cholesterol (Avanti Polar Lipids), and DMG-PEG 2000 (1,2-dimyristoyl-rac-glycero-3-methoxypolyethylene glycol-2000) (Avanti Polar Lipids)[22].

Following formulation, LNPs were diluted 10-fold with PBS and purified using sterilized centrifugal filters with a 10-kilodalton molecular weight cutoff (Amicon, Millipore Sigma) at 4 °C and 2000 x *g* for buffer exchange purpose. The size, PDI, and zeta potential of the LNPs were measured using a Zetasizer Nano (Malvern Instruments) and analyzed with Zetasizer 7.12 software (Malvern Instruments). Encapsulation efficiency and RNA concentration were determined using the Quant-iT RiboGreen RNA Assay Kit (Thermo Fisher Scientific) as previously described[23].

Delivery Systems.

Vibrating membrane nebulizer (CM nebulizer)

The CM Nebulizer was employed using the Pari eFlow (Pari GmbH). The nebulizer reservoir was loaded with 6 mL of either mRNA-LNPs or saRNA-LNPs. The aerosolization process required approximately 15 min to complete, during which the generated aerosol was collected in a 5 mL nuclease-free Eppendorf tube for subsequent LNP characterization. Previous studies have indicated that vibrating membrane nebulizers exhibit a progressive increase in aerosol output over time, likely attributed to the temperature rise within the formulation, caused by vibrational energy dissipation within the nebulizer and reservoir[6].

Commercial nasal spray device (CM spray)

The CM Spray, commonly referred to as a Mucosal Atomization Device (MAD), operates through high-velocity atomization to facilitate intranasal drug delivery. The device reservoir was filled with 200 µL of mRNA-LNPs or saRNA-LNPs. Upon actuation, the device pressurized the liquid formulation through a fine spray nozzle in a second, generating an aerosolized mist composed of micron-sized droplets. The collected aerosol was subsequently transferred into a 5 mL nuclease-free Eppendorf tube for further LNP characterization and experiments.

Laminar fluid ejection (LFE) device

The LFE Device employs a spring-actuated mechanism to deliver a continuous, non-atomized fluid stream through a cannula with an inner diameter of 1.35 mm. The syringe was filled with 200 µL of mRNA-LNPs or saRNA-LNPs. The resulting fluid stream was collected in a 5 mL nuclease-free Eppendorf tube for subsequent LNP characterization and experimental analysis. Unlike conventional nebulization systems that rely on vibration or high-pressure dispersion, the LFE Device maintains laminar flow dynamics (Reynolds number < 2300), ensuring controlled deposition with minimal shear stress. The adjustable ejection velocity (1.1–18.6 m/s – for viscosity 1 cP and 50 cP) allows for targeted fluid delivery while ensuring the fluid remains cohesive, minimizing droplet dispersion and turbulence[12].

Cell lines.

HEK293T Lenti-X cells (Takara Bio, #632180) were maintained at 37 °C in a humidified atmosphere with 5% CO_2. Cells were cultured in Dulbecco's Modified Eagle Medium (DMEM, Thermo Fisher Scientific) supplemented with 10% fetal bovine serum (FBS), 1% GlutaMAX, and 1% penicillin-streptomycin (100 U/mL-100 µg/mL). Additional selective antibiotics were used as required.

Cell Transfection and In Vitro Luciferase Assay.

A total of 10,000 HEK293T cells were seeded per well in a 96-well plate the night before transfection. Following aerosolization, 100 ng of saRNA-Fluc or mRNA-Fluc in LNPs was transfected per well. After 24 h, the cells were lysed, and luciferase activity was quantified using the One-Glo luciferase assay (Promega). The total lysate from each well was transferred to a white 96-well plate (Thermo Fisher Scientific) for analysis and quantified using a TECAN plate reader.

Statistical analysis

Statistical analysis was performed as described in figure legends using GraphPad Prism 10.2.1.

Results

Comparison of delivery mechanisms across different dispensing methods

In this study, lipid nanoparticles (LNP) were formulated using the clinically-approved BNT162b2 LNP[24] composition (Table S1), encapsulating either messenger RNA (mRNA) or self-amplifying RNA (saRNA) (Figure. 1a) and subjected to different delivery devices. After dispensing, the LNPs were collected for characterization and cell transfection. Figure 1 illustrates the RNA-LNP structure, and the three delivery methods used in this study. Figure 1a depicts the mRNA-LNP and saRNA-LNP formulations. In both cases, the RNA contains a gene of interest (GOI) that encodes the firefly luciferase (Fluc) protein, which serves as a reporter for downstream protein quantification assays. The mRNA-Fluc and saRNA-Fluc constructs were composed of 2,111 and 9,451 base pairs, respectively. We chose to include these two types of RNA to observe how device induced mechanical forces affect the integrity of RNA of varying length, which further tailors the future design of RNA-based intranasal delivery systems for therapeutic applications. We first explored the vibrating membrane nebulizer operates by passing LNPs through a perforated membrane containing thousands of micron-sized holes that vibrate at high frequency. The actuator-induced vibration generates a fine LNP aerosol mist with a uniform droplet size, which represents a clinically relevant nebulization technology (Fig. 1b)[13]. We next examined a commercially available nasal spray equipped with a pressurized pump. Upon actuation, the pump generates an aerosol, dispersing LNP formulations into fine droplets typically ranging from 20 to 100 microns in diameter (Fig. 1c)[25]. Finally, we evaluated the laminar fluid ejection (LFE) device, designed to precisely eject fluid through a cannula for targeted deposition at the olfactory cleft. The system utilized a universal 1 mL polycarbonate syringe mounted on a carbon-fiber reinforced mechanism, where a coil spring and orifice-based damper controlled fluid release, ensuring smooth, low-velocity ejections with minimal shear force for efficient intranasal

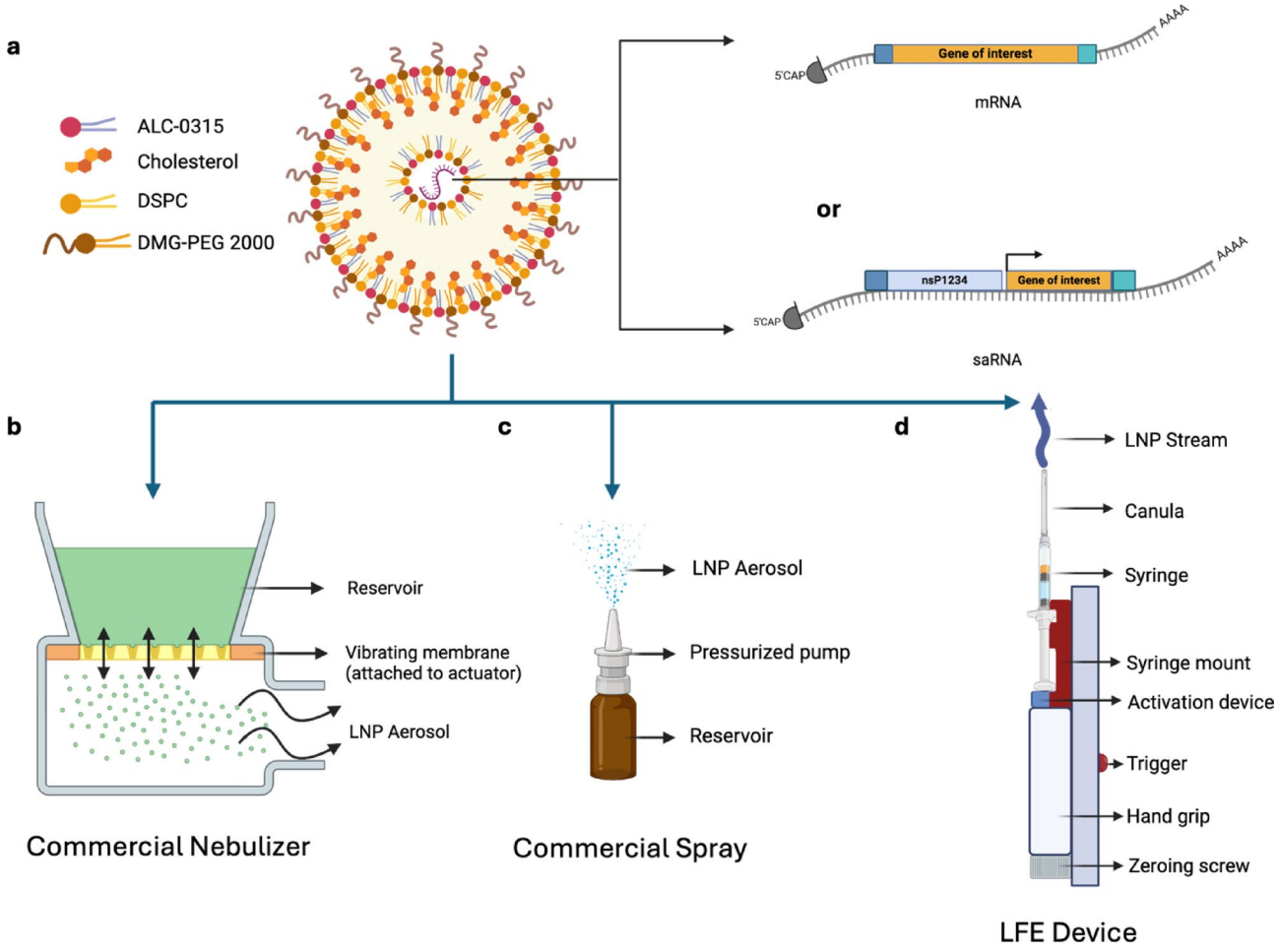

Fig. 1. Illustration of delivery systems used in this study. **(a)** Schematic of LNP with mRNA or saRNA encapsulated **(b)** Vibrating membrane nebulizer (CM Nebulizer): A precision-drilled membrane with thousands of micron-sized holes is mounted on a ring-shaped piezoelectric actuator, which rapidly oscillates the membrane to produce a fine aerosol mist with uniform droplet size. **(c)** Commercial nasal spray (CM Spray): A mechanical pump generates pressure by pressing the nozzle, forcing liquid through a small aperture to produce a fine mist. **(d)** Laminar fluid ejection device (LFE Device): A LFE self-administration tool with an ergonomic introducer for accurate positioning and an interlock mechanism that prevents activation until properly placed, ensuring safe and reliable use. (Created in https://BioRender.com)

delivery (Fig. 1d)[12]. The experimental design aimed to assess whether the mechanical forces created by different nebulizing systems can significantly impact LNP physicochemical properties, leading to RNA degradation and a reduction in protein expression in vitro.

The LFE device maintains LNP size and PDI while the nebulizer increases both after administration

The physicochemical properties of LNPs encapsulating mRNA-Fluc and saRNA-Fluc, including particle size, PDI, and zeta potential, as measured using a dynamic light scattering (DLS) device, were analyzed.

Compared to mRNA and saRNA control LNPs that were not aerosolized, the CM Nebulizer (vibrating membrane) resulted in a significant increase in particle size. In contrast, the LFE Device maintained particle size similar to the control, while CM Spray led to a slight increase in particle size (Fig. 2a and b). The PDI after administration with the CM Nebulizer was significantly higher than the PDI in the CM Spray and the LFE Device, indicating that the CM Nebulizer not only produced larger LNPs but also generated non-uniform droplet output (Fig. 2c and d). High-quality LNPs are typically expected to have a size range of 80–100 nm in diameter and a PDI below 0.2, which indicates uniformity[26]. Figure 2e and f showed that all the LNPs, whether with or without nebulization, exhibited slight negative charge and are near neutral. A previous publication has indicated that a slight negative or neutral zeta potential is beneficial for RNA delivery, as surface charge influences transfection efficiency in cells[27]. Although CM Spray exhibited the most variation in zeta potential results, the aerosolization process across different devices did not result in a significant change of zeta potential of the LNPs. However, the LFE Device consistently demonstrated the comparable particle sizes to both mRNA and saRNA controls and showed the lowest PDI, which then motivated testing with in vitro studies.

Comparison of RNA recovery and encapsulation efficiency on different dispensing methods

The Ribogreen RNA assay was performed to determine the encapsulation efficiency of both RNA within LNPs after delivering with different devices[20,28]. Unlike conventional approaches where RNA encapsulation efficiency is measured immediately after LNP formulation using the Ribogreen assay, our study design involved dispensing the RNA-LNPs first, followed by collection and analysis to assess encapsulation efficiency post-treatment. The encapsulation efficiency of treated samples was then compared to control samples that were measured without undergoing the dispensing process.

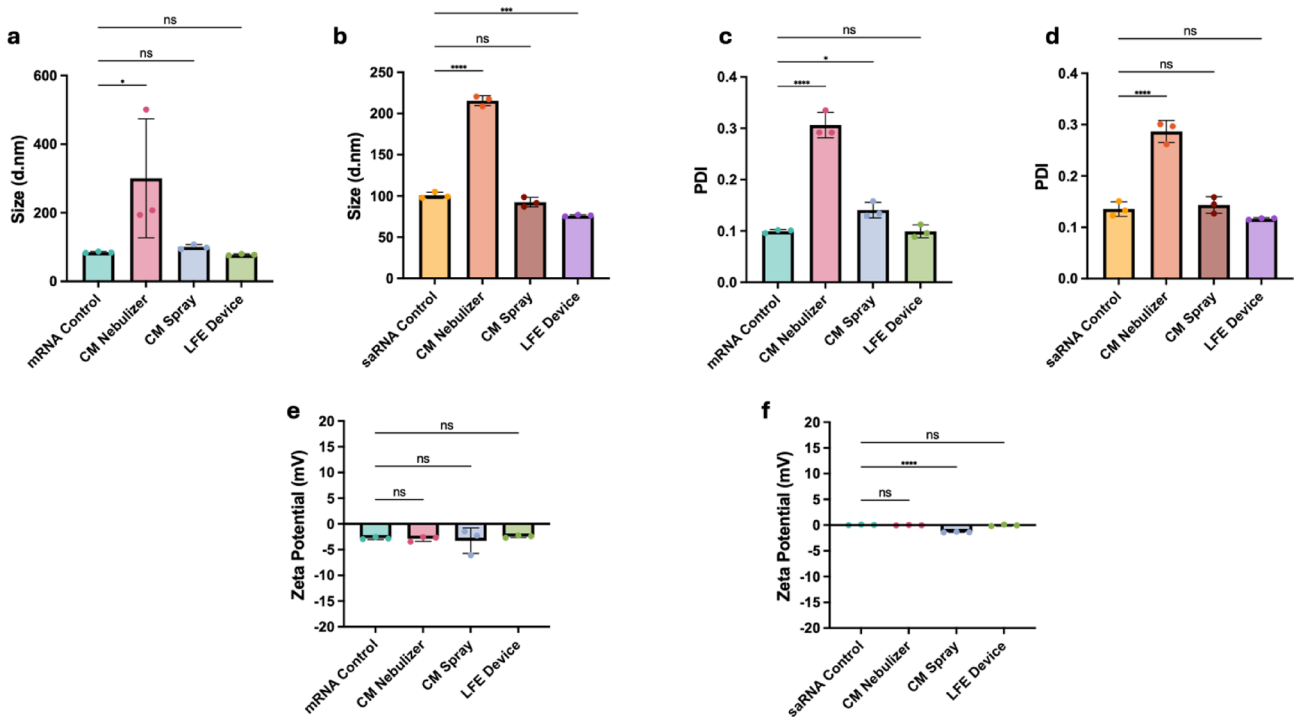

Fig. 2. Physicochemical properties of LNPs encapsulating mRNA-Fluc and saRNA-Fluc, measured using a dynamic light scattering device (Zetasizer Nano, Malvern Instruments). **(a)** Comparison of LNP sizes for mRNA-Fluc and **(b)** saRNA-Fluc after treating with the CM Nebulizer, the CM Spray, and the LFE Device. Polydispersity index of **(c)**mRNA-Fluc and **(d)** saRNA-Fluc after treating with the same devices. Surface charge data from zeta potential (mV) measurements for **(e)** mRNA-Fluc and **(f)** saRNA-Fluc after being treated with the same devices. Data are presented as mean (SD) from $n = 3$ technical replicates and analyzed using one-way ANOVA, followed by Dunnett's multiple comparison test. $^{*}P < 0.05$; $^{**}P < 0.01$; $^{***}P < 0.001$; $^{***}P < 0.0001$; ns – not significant.

We first measured the recovery percentage of RNA-LNP volume by calculating the ratio of output volume to input volume:

$$\text{Recovery Percentage}(\%) = \frac{RNA-LNP\,Volume\,Collected}{Initial\,RNA\_LNP\,Volume\,Filled\,in\,the\,Reservoir}) \times 100\%$$

This measurement provides insight into the amount of dead volume lost during the delivering process. Among all datasets, the CM Nebulizer required the highest input volume (5–6 mL) due to its high dead volume, as indicated in the manufacturer's manual (over 1 mL) while the LFE Device and CM Spray can function with much lower input volumes (200–240 µL). In the mRNA-LNP recovery assessment, the LFE Device demonstrated the highest recovery efficiency, resulting in recovery of ~46% of the input LNP volume. In contrast, the CM Nebulizer exhibited the lowest recovery at ~11%, while the CM Spray recovered ~36% (Fig. 3a). In the saRNA-

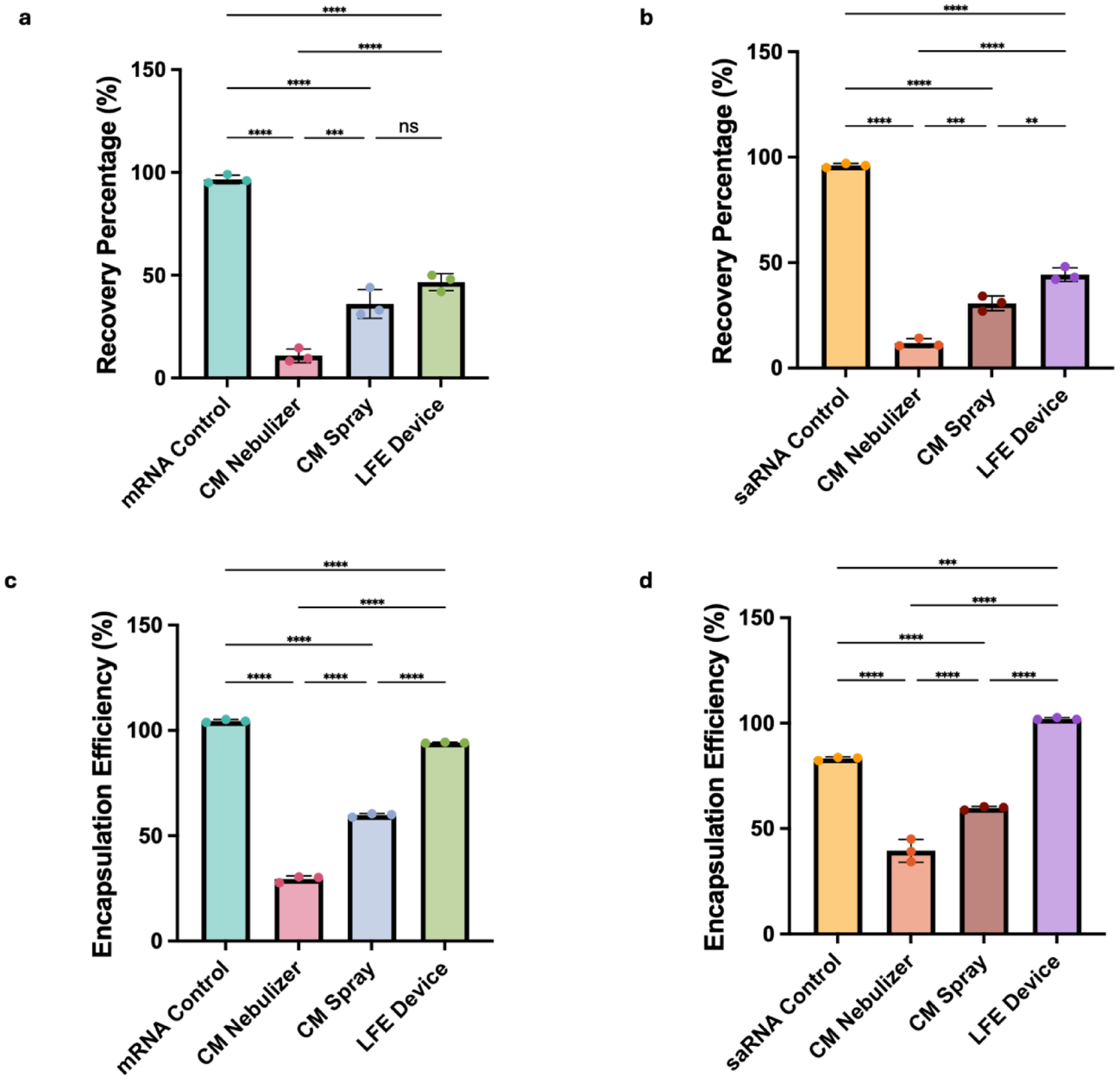

Fig. 3. The RNA-LNP volume recovery in percentage after dispensing and the encapsulation efficiency by Ribogreen fluorescence assay **(a)** mRNA-LNP volume recovery percentage. **(b)** saRNA-LNP volume recovery percentage. **(c)** RNA encapsulation efficiency of mRNA-LNP after treating with the CM Nebulizer, the CM Spray, and the LFE Device. **(d)** RNA encapsulation efficiency of saRNA-LNP after being treated with the same devices. Data are presented as mean (SD) from $n = 3$ technical replicates and analyzed using one-way ANOVA, followed by Dunnett's multiple comparison test. $^{*}P < 0.05$; $^{**}P < 0.01$; $^{***}P < 0.001$; $^{***}P < 0.0001$.

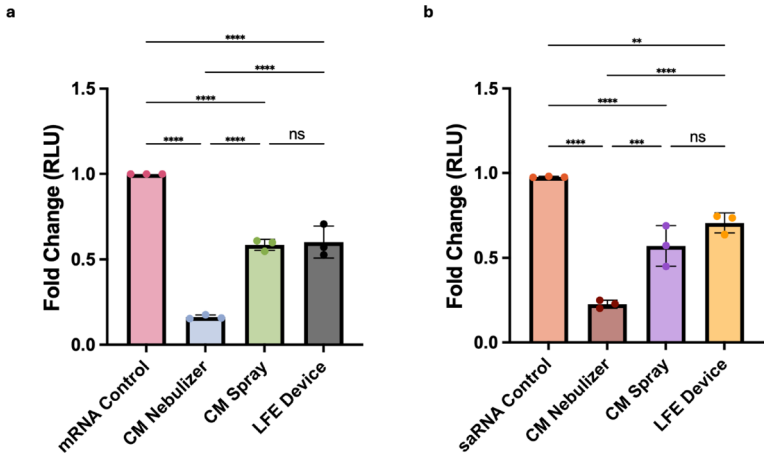

Fig. 4. Relative bioluminescence of HEK293T cells 24 h after transfection. Relative light units after transfection with LNPs containing **(a)** mRNA-Fluc and **(b)** saRNA-Fluc. Bars representing the mean fold change ± standard deviation normalized to mRNA and saRNA control. Data are presented as mean (SD) from $n = 3$ and analyzed using one-way ANOVA, followed by Dunnett's multiple comparison test. $^{*}P < 0.05$; $^{**}P < 0.01$; $^{***}P < 0.001$; $^{***}P < 0.0001$.

LNP measurement, a similar pattern was observed. The LFE Device achieved the highest recovery percentage at ~ 44%, followed by the CM Spray at ~ 31%, while the CM Nebulizer had the lowest recovery at ~ 12% (Fig. 3b).

While the LFE Device outperformed the other tested systems in terms of recovery, it still showed an approximate 50% loss of the input LNP solution. This can likely be attributed to several factors. First, device dead volume and fluid retention within internal components (e.g., tubing, cannula, chamber) can limit full ejection of the payload, reducing measurable recovery. Second, nonspecific adhesion of LNPs to the surfaces of the delivery and collection devices—especially those composed of plastic materials—can result in additional loss. In contrast, control samples were directly pipetted using a needle and collected in low-retention microcentrifuge tubes, minimizing both dead volume and adhesion losses and thereby achieving nearly complete recovery. Additionally, as the input volume increases, the impact of dead volume on recovery percentage is expected to diminish for the LFE Device, which may lead to improved recovery efficiency in scaled-up applications.

We then characterized the encapsulation efficiency using the following equation:

$$\text{Encapsulation Efficiency}(\%) = \left(\frac{Amount\ of\ Encapsulated\ RNA}{Amount\ of\ Total\ RNA} \right) \times 100\%$$

The LFE Device produced LNPs with an encapsulation efficiency (EE) of ~ 94%, whereas the CM Nebulizer resulted in a significantly lower EE of ~ 29%, and the CM Spray achieved ~ 60% EE (Fig. 3c). There was a similar pattern in the saRNA dataset; the LFE Device demonstrated an EE of ~ 102%, while the CM Nebulizer and CM Spray yielded ~ 39% and ~ 59% EE, respectively (Fig. 3d). In the saRNA encapsulation efficiency (EE) experiment, the LFE Device exhibited an EE exceeding 100%, surpassing the saRNA control. We hypothesize that the low-shear-force dispensing process in the LFE Device may induce lipid reorganization, enhancing interactions with longer saRNA fragments compared to the non-nebulized control. A previous study reported that lower shear force aerosolization can prevent encapsulated mRNA from leaking, preserving RNA integrity[29]. However, further experiments are required to validate this hypothesis.

The LFE Device demonstrated a higher recovery rate, achieving ~ 46% for mRNA-LNP and ~ 44% for saRNA-LNP, compared to the CM Nebulizer, which recovered only ~ 11% for mRNA-LNP and ~ 12% for saRNA-LNP, and the CM Spray, which achieved ~ 36% for mRNA-LNP and ~ 31% for saRNA-LNP. In terms of EE, the LFE Device achieved ~ 94% for mRNA-LNP and ~ 102% for saRNA-LNP, significantly outperforming the CM Nebulizer (~ 29% for mRNA-LNP, ~ 39% for saRNA-LNP) and the CM Spray (~ 59% for both mRNA-LNP and saRNA-LNP). These results, combined with physicochemical characterization data, suggest that the strong shear forces generated by the CM Nebulizer and CM Spray may have disrupted the RNA-LNP structure during the aerosolization process, leading to increased particle sizes, higher PDI, and reduced RNA EE.

In vitro biological activity of delivered RNA-LNP

We investigated the biological activity of delivered mRNA-LNP and saRNA-LNP using RNA encoding firefly luciferase and transfecting HEK293T cells and quantifying the resulting bioluminescence after 24 h of transfection. With the LFE Device ejected mRNA-LNPs, luciferase functional protein expression reached 60% relative to the mRNA control, whereas the CM Nebulizer resulted in a significantly lower expression level of 16%, and CM Spray resulted in a similar expression level of 58% (Fig. 4a). Similarly, in the saRNA dataset, the LFE Device achieved 70% of the functional luciferase protein expression compared to the saRNA control, while the CM Nebulizer and CM Spray resulted in 23% and 57%, respectively (Fig. 4b). Among the delivery systems, the CM Nebulizer exhibited the lowest relative luminescence units (RLU), whereas the CM Spray and the LFE

Device demonstrated comparable expression levels. In the saRNA experiments, the LFE Device yielded the highest RLU, followed by the CM Spray, while the CM Nebulizer produced the lowest bioluminescence signal, indicating the greatest loss of functional RNA post-aerosolization.

Discussion

In this study, we evaluated the impact of three drug delivery systems- CM Nebulizer, CM Spray, and LFE Device- on the physiochemical properties, RNA-LNP recovery percentage, RNA EE, and biological activity of RNA-LNP formulations. Our findings revealed significant differences in RNA-LNP stability and device recovery among these delivery systems.

The CM Nebulizer notably increased LNP particle size from an average 85 nm to 300 nm and raised the PDI from 0.1 to 0.3, suggesting substantial structural disruption due to higher shear forces. In contrast, the LFE Device not only maintained the particle size well, but had the lowest PDI change (0.099 for mRNA, 0.117 for saRNA), indicating superior LNP stability. To further evaluate LNP retention during drug delivery, we measured RNA-LNP recovery by comparing collected output to the initial reservoir volume. The LFE Device achieved the highest recovery (46% of mRNA-LNP and 44% for saRNA-LNP), whereas the CM Nebulizer exhibited the lowest (11–12% for both RNA-LNPs), underscoring variations in nebulization efficiency. EE was also highest in the LFE Device (94% for mRNA, 102% for saRNA), and lowest in the CM Nebulizer (29% and 39%, respectively). Consistently, functional protein expression analysis further supported these trends, with the LFE Device yielding 60% and 70% luciferase protein expression for mRNA and saRNA, compared to significantly lower levels in the CM Nebulizer (16% in mRNA, 23% in saRNA). Taken together, our results demonstrate that the LFE Device preserves LNP structural integrity, maintains a small and uniform particle size, minimizes dead volume loss, ensures high RNA encapsulation efficiency, and enhances functional protein expression.

In the post-pandemic era, scientists are actively working to prevent future respiratory infectious diseases like SARS-CoV-2. Mucosal vaccines have emerged as a promising strategy, as they can elicit robust immune responses at the mucosal surfaces-the primary entry points for respiratory pathogens. Unlike traditional injectable vaccines, mucosal vaccines have the potential to prevent infections from establishing rather than mitigating the symptoms[30]. Nebulization-based intranasal vaccine delivery is an efficient strategy for respiratory applications. However, the impact of different nebulization systems on RNA integrity and the subsequent immune response remains unclear. Previous studies addressed the issue of high shear forces leading to the disruption of LNPs and degradation of the encapsulated mRNA[6,8]. To address this, they introduce a novel low-energy nebulization approach utilizing a nanotech membrane to significantly reduce energy dissipation during aerosol generation thereby preserving both the LNP structure and mRNA integrity[6].

Our findings are in agreeance with these studies, demonstrating that high mechanical stresses (such as shear forces) in intranasal delivery systems can significantly impact RNA-LNP stability and functionality. Specifically, luciferase protein expression results in our study illustrate how structural alterations influence biological activity. Furthermore, the LFE Device, which operates with lower mechanical stress forces, preserved RNA-LNP integrity more effectively and had higher protein expression than the CM Nebulizer. Additionally, while previous studies primarily focused on mRNA-LNPs, our study expands this understanding by incorporating saRNA-LNPs. The superior encapsulation efficiency preservation and protein expression observed in the LFE Device-treated saRNA-LNPs suggest that lower shear forces also facilitate saRNA retention and stability during the delivery process. This is particularly relevant given the growing interest in saRNA-based vaccines, which require careful formulation to ensure the optimal delivery and efficacy[14,31]. Additionally, although the CM Spray exhibited lower RNA encapsulation efficiency than the LFE Device, comparable levels of luciferase protein expression were observed because transfection experiments were normalized to the same amount of encapsulated RNA (100 ng) following quantification after aerosolization. This normalization allowed us to directly assess the functional RNA delivered, independent of total encapsulation differences.

Despite these promising findings, our study has limitations. First, while we demonstrated the physicochemical stability and functional protein expression of nebulized RNA-LNPs in vitro, further in vivo studies are necessary to evaluate immune responses and mucosal delivery efficiency. Second, our study focused on a single formulation based on the clinically approved BNT162b2 LNP composition; future work should explore additional lipid compositions and formulations optimized for intranasal administration. Moreover, there are studies showing that viscosity can play a crucial role in intranasal delivery and deposition, and potentially affect the droplet size[32,33]. Additionally, although our results suggest that LNPs may undergo structural reformation during the delivery process, further mechanistic studies using advanced imaging techniques, such as transmission electron microscopy (TEM), are needed to directly visualize these changes. Additionally, direct assessment of RNA integrity by capillary electrophoresis was not performed in this study. Since RNA is encapsulated within LNPs, additional extraction steps would be required before analysis, which can introduce variability and potential degradation. Therefore, functional output measurements such as luciferase expression were prioritized to evaluate RNA stability in this initial evaluation. However, methods for RNA extraction and capillary electrophoresis protocols are currently in development, particularly tailored for large and structurally complex saRNA, to enable more detailed molecular characterization in future studies.

Overall, our findings highlight the importance of selecting an appropriate delivery system for RNA-LNP intranasal delivery. The LFE Device consistently preserved LNP integrity, maximized encapsulation efficiency, and achieved superior protein expression while minimizing the LNP dead volume. These insights contribute to the development of effective intranasal RNA-LNP delivery strategies, with potential applications in next-generation mucosal vaccines and therapeutic RNA formulations.

Data availability

The data that support the findings of this study are available from the corresponding author (A.K.B.), upon reasonable request.

Received: 8 April 2025; Accepted: 20 May 2025
Published online: 27 May 2025

References

1. Ashraf, M. U. et al. COVID-19 vaccines (revisited) and oral-mucosal vector system as a potential vaccine platform. *Vaccines* **9**(2). https://doi.org/10.3390/vaccines9020171 (2021).
2. Lund, F. E. & Randall, T. D. Scent of a vaccine. *Science* **373**(6553), 397–399. https://doi.org/10.1126/science.abg9857 (2021).
3. Afkhami, S. et al. Mar., Respiratory mucosal delivery of next-generation COVID-19 vaccine provides robust protection against both ancestral and variant strains of SARS-CoV-2, *Cell* **185**(5), 896–915.e19. https://doi.org/10.1016/j.cell.2022.02.005 (2022).
4. Baldeon Vaca, G. et al. Sep., Intranasal mRNA-LNP vaccination protects hamsters from SARS-CoV-2 infection, *Sci. Adv.*, vol. 9, no. 38, p. eadh1655, (2023). https://doi.org/10.1126/sciadv.adh1655
5. Reichmuth, A. M., Oberli, M. A., Jaklenec, A., Langer, R. & Blankschtein, D. mRNA vaccine delivery using lipid nanoparticles. *Ther. Deliv.* **7**(5), 319–334. https://doi.org/10.4155/tde-2016-0006 (2016).
6. van Rijn, C. J. M. et al. Low energy nebulization preserves integrity of SARS-CoV-2 mRNA vaccines for respiratory delivery. *Sci. Rep.* **13**(1), 8851. https://doi.org/10.1038/s41598-023-35872-4 (2023).
7. Adam, R. E. & Zimm, B. H. Shear degradation of DNA*. *Nucleic Acids Res.* **4**(5), 1513–1538. https://doi.org/10.1093/nar/4.5.1513 (1977).
8. Coleman, H. et al. Effect of mechanical stresses on viral capsid disruption during droplet formation and drying. *Colloids Surf. B Biointerfaces*. **233**, 113661. https://doi.org/10.1016/j.colsurfb.2023.113661 (2024).
9. Hou, H. et al. Applications and research progress of traditional Chinese medicine delivered via nasal administration. *Biomed. Pharmacother.* **157**, 113933. https://doi.org/10.1016/j.biopha.2022.113933 (Jan. 2023).
10. Bronsky, E. A. et al. May., A clinical trial of ipratropium bromide nasal spray in patients with perennial nonallergic rhinitis, *J. Allergy Clin. Immunol.*, vol. 95, no. 5 Pt 2, pp. 1117–1122, (1995). https://doi.org/10.1016/s0091-6749(95)70215-6
11. Lam, J. K. W. et al. Transmucosal drug administration as an alternative route in palliative and end-of-life care during the COVID-19 pandemic. *Adv. Drug Deliv Rev.* **160**, 234–243. https://doi.org/10.1016/j.addr.2020.10.018 (2020).
12. Morin, T. M. et al. Laminar fluid ejection for olfactory drug delivery: A proof of concept study. *IEEE J. Transl Eng. Health Med.* **12**, 727–738. https://doi.org/10.1109/JTEHM.2024.3503498 (2024).
13. Lass, J. S., Sant, A. & Knoch, M. New advances in aerosolised drug delivery: vibrating membrane nebuliser technology. *Expert Opin. Drug Deliv.* **3**(5), 693–702. https://doi.org/10.1517/17425247.3.5.693 (2006).
14. Casmil, I. C. et al. Alphaviral backbone of self-amplifying RNA enhances protein expression and immunogenicity against SARS-CoV-2 antigen. *Mol. Ther.* **33**(2), 514–528. https://doi.org/10.1016/j.ymthe.2024.12.055 (2025).
15. Pietilä, M. K., Hellström, K. & Ahola, T. Alphavirus polymerase and RNA replication. *Virus Res.* **234**, 44–57. https://doi.org/10.1016/j.virusres.2017.01.007 (2017).
16. Vogel, A. B. et al. Self-Amplifying RNA vaccines give equivalent protection against influenza to mRNA vaccines but at much lower doses. *Mol. Ther.* **26**(2), 446–455. https://doi.org/10.1016/j.ymthe.2017.11.017 (2018).
17. Oda, Y. et al. Persistence of immune responses of a self-amplifying RNA COVID-19 vaccine (ARCT-154) versus BNT162b2. *Lancet Infect. Dis.* **24**(4), 341–343. https://doi.org/10.1016/S1473-3099(24)00060-4 (2024).
18. Amplifying mRNA vaccine approved. *Nat. Biotechnol.* **42**(1), 4–4. https://doi.org/10.1038/s41587-023-02101-2 (2024).
19. Bathula, N. V. et al. Oct., Delivery vehicle and route of administration influences self-amplifying RNA biodistribution, expression kinetics, and reactogenicity. *J. Controlled Release* **374**, 28–38. https://doi.org/10.1016/j.jconrel.2024.07.078 (2024).
20. Ly, H. H., Daniel, S., Soriano, S. K. V., Kis, Z. & Blakney, A. K. Optimization of lipid nanoparticles for saRNA expression and cellular activation using a design-of-experiment approach. *Mol. Pharm.* **19**(6), 1892–1905. https://doi.org/10.1021/acs.molpharmaceut.2c00032 (2022).
21. Popova, P. G., Lagace, M. A., Tang, G. & Blakney, A. K. Effect of *in vitro* transcription conditions on yield of high quality messenger and self-amplifying RNA. *Eur. J. Pharm. Biopharm.* **198**, 114247. https://doi.org/10.1016/j.ejpb.2024.114247 (2024).
22. Tenchov, R., Bird, R., Curtze, A. E. & Zhou, Q. Lipid nanoparticlesfrom liposomes to mRNA vaccine delivery, a landscape of research diversity and advancement. *ACS Nano* **15**(11), 16982–17015. https://doi.org/10.1021/acsnano.1c04996 (2021).
23. Blakney, A. K., McKay, P. F., Yus, B. I., Aldon, Y. & Shattock, R. J. Inside out: Optimization of lipid nanoparticle formulations for exterior complexation and in vivo delivery of saRNA, *Gene Ther.* **26**(9), 363–372. https://doi.org/10.1038/s41434-019-0095-2 (2019).
24. Schoenmaker, L. et al. mRNA-lipid nanoparticle COVID-19 vaccines: structure and stability. *Int. J. Pharm.* **601**, 120586. https://doi.org/10.1016/j.ijpharm.2021.120586 (2021).
25. Rygg, A., Hindle, M. & Longest, P. W. Absorption and clearance of pharmaceutical aerosols in the human nose: Effects of nasal spray suspension particle size and properties. *Pharm. Res.* **33**(4), 909–921. https://doi.org/10.1007/s11095-015-1837-5 (2016).
26. Roces, C. B. et al. Manufacturing considerations for the development of lipid nanoparticles using microfluidics. *Pharmaceutics* **12**(11), 11. https://doi.org/10.3390/pharmaceutics12111095 (2020).
27. Chen, H., Ren, X., Xu, S., Zhang, D. & Han, T. Optimization of lipid nanoformulations for effective mRNA delivery. *Int. J. Nanomed.* **17**, 2893–2905. https://doi.org/10.2147/IJN.S363990 (2022)
28. Blakney, A. K., McKay, P. F., Yus, B. I., Aldon, Y. & Shattock, R. J. Inside out: optimization of lipid nanoparticle formulations for exterior complexation and in vivo delivery of SaRNA. *Gene Ther.* **26**(9), 363–372. https://doi.org/10.1038/s41434-019-0095-2 (2019).
29. Kim, J. et al. Microfluidic platform enables shearless aerosolization of lipid nanoparticles for mRNA inhalation. *ACS Nano*. **18**, 11335–11348. https://doi.org/10.1021/acsnano.4c00768 (2024).
30. Lavelle, E. C. & Ward, R. W. Mucosal vaccines—fortifying the frontiers. *Nat. Rev. Immunol.* **22**(4), 236–250. https://doi.org/10.1038/s41577-021-00583-2 (2022).
31. Hồ, N. T. et al. Safety, immunogenicity and efficacy of the self-amplifying mRNA ARCT-154 COVID-19 vaccine: Pooled phase 1, 2, 3a and 3b randomized, controlled trials. *Nat. Commun.* **15**(1), 4081. https://doi.org/10.1038/s41467-024-47905-1 (2024).
32. Gao, M., Shen, X. & Mao, S. Factors influencing drug deposition in thenasal cavity upon delivery via nasal sprays. *J. Pharm. Investig.* **50**(3), 251–259. https://doi.org/10.1007/s40005-020-00482-z (2020).
33. Kundoor, V. & Dalby, R. N. Effect of formulation- and administration-related variables on deposition pattern of nasal spray pumps evaluated using a nasal cast. *Pharm. Res.* **28**(8), 1895–1904. https://doi.org/10.1007/s11095-011-0417-6 (2011).

Author contributions

C.H.H., I.C.C., M.S., T.R., K.E., N.A. and A.K.B. designed experiments, C.H.H., I.C.C., and M.S. executed experiments, collected and analyzed data, C.H.H. wrote the manuscript with editing and revisions from I.C.C., M.S., T.R., K.E., N.A. and A.K.B.

Funding
This work was supported by the Natural Sciences and Engineering Research Council of Canada, the Canadian Institutes of Health Research, research funding from Rocket Science Health, a Tier II Canada Research Chair and a Michael Smith Health Research BC Scholar Award to A.K.B.

Declarations

Competing interests
This work was funded in part by Rocket Science Health (RSH), and M.S., T.R., K.E., and N.A. are employees of RSH. The other authors have no competing interests to declare.

Additional information
Supplementary Information The online version contains supplementary material available at https://doi.org/10.1038/s41598-025-03309-9.

Correspondence and requests for materials should be addressed to A.K.B.

Reprints and permissions information is available at www.nature.com/reprints.

Publisher's note Springer Nature remains neutral with regard to jurisdictional claims in published maps and institutional affiliations.